Transmission of order in a correlated spin glass

Adler, Joan; Enter, Aernout C.D. van; Harris, A.B.

Published in:
Physical Review. B: Condensed Matter and Materials Physics

Publication date:
1988

Transmission of order in a correlated spin glass

Joan Adler
School of Physics and Astronomy, Tel Aviv University, 69978 Tel Aviv, Israel
and Department of Physics, Technion-ITT, 32000 Haifa, Israel

Aernout C. D. van Enter
Department of Physics, Technion-ITT, 32000 Haifa, Israel

A. B. Harris
School of Physics and Astronomy, Tel Aviv University, 69978 Tel Aviv, Israel
and Department of Physics, University of Pennsylvania, Philadelphia, Pennsylvania 19104
(Received 8 June 1988)

We introduce a new family of models for spin-glass systems. This family has quenched site dilution with varying strengths of local correlations and modulated ordered phases in the pure limit. The correlated dilution mimics the experimental situation in Cu-Mn, Au-Fe, and Pt-Mn. Relatively weak correlations are conjectured to be sufficient to explain the observed interactions between regions of modulated spin order and coexisting smaller ferromagnetic regions in CuMn. The models are investigated by the transmission-of-order approach, which relates the zero-temperature line of the temperature-dilution phase diagram to a family of correlated percolation models. Exact results for the correlated percolation models on the Cayley tree and simulations on the square lattice are presented. We find novel phases in which percolation occurs on some but not all sublattices.

I. INTRODUCTION

There are many features of real spin glasses[1] such as Cu-Mn that most model systems do not include or reproduce. Some features that are not included relate to the nature of the randomness. In particular, most models have independently distributed randomness neglecting thereby the compositional correlations in the randomness which are present[2] in some real spin glasses. The main aim of this paper is to investigate whether or not such correlations can lead to qualitatively important effects. For the case of a diluted ferromagnet, one can immediately dismiss this possibility. However, in spin glasses where there are competing interactions, we find that such correlations can drastically modify the nature of the phase diagram. In the present paper we will elucidate this phenomenon by analyzing a rather simplified model which is amenable to study via both numerical and analytic means. There are other possible manifestations of compositional correlations which we will not consider in depth here. Among these is the interplay between longer-ranged modulated regions and shorter-ranged ferromagnetic regions are observed by Cable *et al.*,[3] and the sharp increase in the susceptibility that occurs near the second-neighbor percolation threshold[4] in Pt-Mn, Au-Mn, and Au-Fe.

We note as well that most models do not allow for the fact that many real spin glasses have complicated multisublattice ordered structure for high concentration of magnetic species. Our model, even though simple, can describe such phenomenology.

Our approach is as follows. We introduce simple models in terms of Ising spins which (a) incorporate the frustration typical of spin-glass systems and (b) permit us to study the effect of frustration combined with correlated dilution. For simplicity, we consider a model system in which frustration only occurs within planes parallel to the x-y plane. Accordingly, spins in adjacent x-y planes on a cubic lattice are ferromagnetically coupled to one another. In the present paper we will confine our analysis to a determination of the phase diagram at zero temperature T as a function of the average concentration of magnetic spins, p, and the degree of correlations in the dilution, described by a nearest-neighbor Ising lattice gas with a correlation parameter K, which we define below. In view of the ferromagnetic coupling between planes, the ground state is determined by the configuration of spins within a single x-y plane. The ferromagnetic coupling between planes is introduced mainly to stabilize the system and we do not suggest that a three-dimensional model with spatial anisotropy is a realistic model for a directionally isotropic spin glass. To treat the frustration we consider two models, both with ferromagnetic interactions between nearest neighbors.[5] The so-called biaxial next-nearest-neighbor Ising, or BNNNI,[6] model has antiferromagnetic interactions between second-nearest neighbors in either the x or y directions. The other model which we will refer to as the planar next-nearest neighbor Ising, or PNNNI, model has antiferromagnetic interactions between next-nearest neighbors. These models are shown in Fig. 1. In either case we consider the limit when the antiferromagnetic interactions dominate. To determine the phase diagram when such systems are diluted at $T=0$, we apply the transmission-of-order approach introduced by Adler *et al.*[7] to model the analogous glasslike behavior[8] of ortho-para hydrogen mixtures at $T=0$. In this ap-

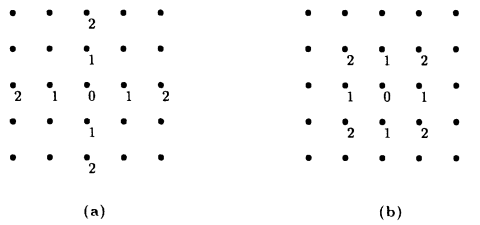

FIG. 1. Interactions in the x-y plane of (a) the BNNNI model and (b) the PNNNI model. In each case an arbitrarily chosen site (labeled 0) is coupled via an exchange interaction J_1 to its nearest neighbors (labeled 1) and via J_2 to a shell of further neighbors (labeled 2).

proach the ordering problem at $T=0$ is replaced by an approximately equivalent multisublattice correlated percolation problem. We will show that for randomness with sufficiently strong correlations, the percolation threshold becomes an interval in concentration of nonzero width in which percolation takes place within some, but not all, sublattices. The existence of such a region of partial percolation follows both from the exact solution of a model for correlated percolation on a Cayley tree, and also from Monte Carlo simulation of the model on a two-dimensional lattice. It is the existence of these novel partially percolating phases which is the main focus and result of this paper. We outline the implications of this result for the BNNNI model and devote the remainder of the present paper to providing evidence to support this proposal. The study of this model at nonzero temperature is deferred to a later paper.

A preliminary account of some of our ideas has already been presented.[9] Certain aspects of correlated percolation that are studied in this work have previously been considered by Murata,[10] in a Cayley-tree calculation for a repulsive lattice gas. These ideas are extended and presented more clearly in the ϵ-expansion calculation of Coniglio and Lubensky,[11] with applications to the sol-gel transition in polymers. To the best of our knowledge the present calculation is the first to consider the effects of correlations on sublattice percolation and we believe that the application of these ideas to spin glasses is entirely novel.

Briefly, this paper is organized as follows. In Sec. II we describe the simple model we wish to study in order to include the effect of compositional correlations mentioned above. Here we discuss some qualitative features of this and similar models. In Sec. III we develop an exact solution for this model on a Cayley tree from which we can obtain the nature of the compositional correlations and also the percolative behavior within each sublattice. Inasmuch as this solution is identified with that for high spatial dimension d, it represents a mean-field solution for this correlated percolation problem. In Sec. IV we give a Hamiltonian formulation, using it to discuss the nature of the resulting field-theoretic description of this problem. In Sec. V we present some results of numerical simulations which elucidate the difference between mean-field behavior and that occurring in $d=2$ dimensions. These results indicate that several interesting questions remain to be studied. Finally, in Sec. VI we summarize our results and the conclusions to be drawn therefrom.

II. MODELS

The Hamiltonian for the BNNNI and PNNNI models on a simple cubic or square lattice can be written as

$$\mathcal{H}=-J_1\sum_{i,j}s_is_j+J_2\sum_{i,j}s_is_j-J^{\perp}\sum_{i,j}s_is_j\ , \tag{1}$$

where s_i is an Ising-spin variable which can assume the values ±1 and the first sum is over pairs of nearest neighbors in the x-y plane and the second is over pairs of second nearest neighbors in the x-y plane in the case of the PNNNI model and over pairs of third nearest neighbors in the x-y plane in the case of the BNNNI model (see Fig. 1). The third sum is over nearest neighbors in the z direction. For the square lattice $J^{\perp}=0$. For $J_2>J_1/2$ the ground state of the pure BNNNI model is the same as that for $J_1=0$, i.e., modulated antiferromagnetic, whereas for the diluted system the situation is more complicated, as we shall see. One may also define three-dimensional versions of these models with antiferromagnetic interactions along all three axis directions or along a [1,1,1] direction. A related competing-interaction model, with nearest-neighbor ferromagnetic and second-neighbor antiferromagnetic interactions between Heisenberg spins,[12] has been extensively studied at low temperatures using spin-wave theory. Such a system was shown[13] to model successfully many qualitative aspects of the full phase diagram of the insulating spin glass $Eu_xSr_{1-x}S$. For the collinear spin structures studied here, it is possible that the phase diagrams in the $p-K$ plane for Ising and Heisenberg spin systems are quite similar to one another.

Any realistic model for metallic spin glasses will have to take into account the longer-ranged exchange interactions of the metallic system in order to obtain quantitative agreement with the experimental phase diagram. Thus we do not claim that a simple model like the BNNNI system will give a quantitative picture. However, we do suggest that such a model with correlated site dilution that mimics the dilution of the Cu, Au, and Pt host matrices by the ferromagnetic Mn and Fe will give qualitative features that have not been explained successfully by most extant models. The qualitative features are specific to metallic glasses and thus need not and cannot be explained by models with interaction parameters discussed in Ref. 13. The extension of our approach to more realistic systems should not require more computational effort than other numerical calculations for spin glasses and could be considerably more efficient.

We now give a heuristic discussion of the phase diagram of the BNNNI model for $J_2>J_1/2$ as a function of concentration. We begin with a discussion of the model in the absence of dilution. We may view this model as having four sublattices within each of which there is long-range antiferromagnetic ordering. (Each of these sublattices could be further decomposed into two ferromagnetic sublattices. Thus one could consider the sys-

tem to have eight sublattices.) Within a given sublattice there are two antiferromagnetic ground states corresponding to two choices of phase. In the absence of dilution, changing the phase within a given sublattice does not affect the energy. Thus since the phase can be chosen arbitrarily on each of the four sublattices, the undiluted

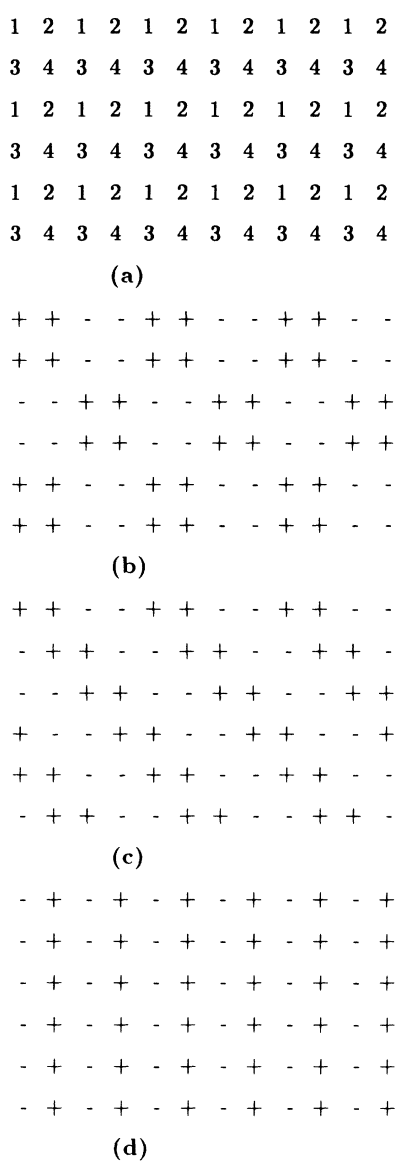

FIG. 2. The pure BNNNI and PNNNI ground states. (a) The four antiferromagnetic sublattices of the BNNNI model, each of which can have an independent phase in its wave function. These phases are indicated by the vector $(\phi_1,\phi_2,\phi_3,\phi_4)$, with $\phi_i = +$ or $-$. (b) One of the eight checkerboard configurations. The choice of phases in this figure is $(+,+,+,+)$. (c) One of the eight staircase configurations. The choice of phases in this figure is $(+,+,-,+)$. (d) One of the two "vertical" ground states of the PNNNI model. (In the two "horizontal" states there are horizontal rows of parallel spins.) For the PNNNI model the two sublattices on which the phase of the antiferromagnetic wave function can be chosen independently are (i) the union of sublattices 1 and 4, and (ii) the union of sublattices 2 and 3 of the BNNNI model in panel (a).

model has $2^4 = 16$ possible ground states, some of which are shown in Fig. 2. There are eight "checkboard" states, as in Fig. 2(b), and eight "staircase" states, as in Fig. 2(c). A similar discussion shows that the PNNNI model may be viewed as having two sublattices and, when undiluted, four ground states. In two of these ground states there are vertical rows of parallel spins and in the other two horizontal rows of parallel spins. We refer to these two ground states as "vertical" and "horizontal," respectively.

If a quenched random dilution of magnetic sites is introduced, then the degeneracy between the different ground states is lifted locally and the uncorrelated dilution acts like a random exchange coupling between sublattices. To see this, we treat the PNNNI model and consider the intersublattice interaction caused by removing (a) a single site and (b) two nearest-neighboring sites, as shown in Fig. 3. In the first case it is easily seen that no net exchange field is induced on either sublattice. However, when a pair of nearest-neighboring sites is removed, an interaction between sublattices is induced and the degeneracy between ground states is lifted, as shown in Fig. 3.

Slightly above the percolation threshold this random interaction can destroy the long-range order as would happen in a similar way in a diluted spin glass,[14] or in the diluted axial next-nearest-neighbor Ising (ANNNI) model.[15] Here we give an Imry-Ma[16] argument to show that uncorrelated random dilution will destroy the long-range

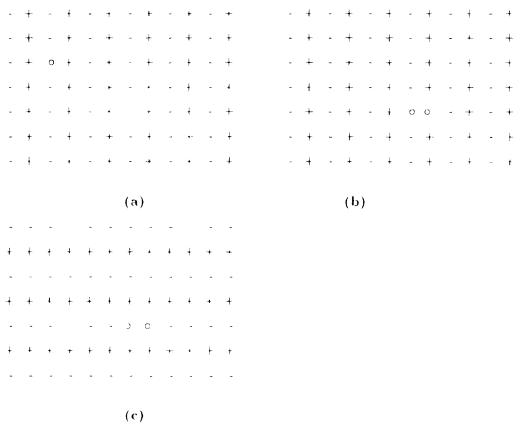

FIG. 3. Local effect of dilution in the PNNNI model. (a) Removing a single site deletes two ferromagnetic and two antiferromagnetic nearest-neighbor interactions for either the "vertical" state, shown here, or for the "horizontal" state, not shown. Thus the "vertical" and "horizontal" states have the same energy, and removal of a single site does not introduce an exchange coupling between sublattices. Removing a horizontal pair of neighboring sites deletes 4 ferromagnetic and 3 antiferromagnetic nearest-neighbor interactions for the "vertical" state [panel (b)] and 3 ferromagnetic and 4 antiferromagnetic interactions for the "horizontal" state [panel (c)]. Thus, removal of a horizontal pair of sites causes the "horizontal" state to have lower energy than the "vertical" state. When a vertical pair of sites is removed, the "vertical" state has the lower energy. Thus, the random occurrence of pairs of vacant sites leads to a random exchange coupling between sublattices.

order in two dimensions ($J^{\perp}=0$). For this argument we consider a domain of size R and estimate the energy of a configuration in which the relative orientation of the two sublattices is reversed inside this domain. By so doing we typically gain a random exchange energy (from pairs removed) of order $-J_1 R^{d/2}$. We also must take account of the concomitant surface energy caused by reversing part of a sublattice. This energy is proportional to the surface area, i.e., it is of order $J_1 R^{d-1}$. For $d \leq 2$, $J^{\perp}=0$, we see that local reversals within a single sublattice are favored for sufficiently large R. Thus for $d \leq 2$ the PNNNI model exhibits no long-range order for any nonzero dilution. This conclusion can be extended to the BNNNI model.

Next we discuss the case of *correlated* dilution, where the situation is quite different. We describe correlated dilution with an Ising lattice gas in the usual way. We introduce site occupation variables ϵ_i ($\epsilon_i=0$ if site i is vacant and $\epsilon_i=1$ if it is occupied), and a chemical potential μ in terms of which we construct the probability $P(\{\epsilon_i\})$ that any configuration of occupied sites occur:

$$P(\{\epsilon_i\})=\frac{e^{K\sum_{\langle i,j\rangle}\epsilon_i\epsilon_j+\mu\sum_i\epsilon_i}}{\sum_{\{\epsilon_i\}} e^{K\sum_{\langle i,j\rangle}\epsilon_i\epsilon_j+\mu\sum_i\epsilon_i}}, \tag{2}$$

where $\sum_{\langle i,j\rangle}$ indicates a sum over *pairs* of nearest-neighboring sites i,j. If we set $K=K_0/(k_B T_A)$, then T_A represents the annealing temperature from which the system was quenched to low temperature, and K_0 the repulsive energy associated with pairs of nearest neighbors. One can relate the average concentration p of occupied sites to μ in the usual way. Alternatively, one can restrict the ϵ_i's in Eq. (2) to satisfy $\sum_i \epsilon_i = pN$, where N is the total number of sites in the system.

Initially we consider the PNNNI model for $K=\infty$ and $p=\frac{1}{2}$. In this case one of the two sublattices is fully occupied and the other is completely vacant. Then there is no random exchange field at all. More generally we see that the Imry-Ma argument does not apply when the correlations become sufficiently strong. In this limit, as we shall see, long-range order does occur in the PNNNI model for $d=2$ ($J^{\perp}=0$).

We now discuss the expected behavior of the BNNNI model with *correlated* dilution ignoring the effect of the random exchange interactions discussed above. We observe that there cannot be long-range magnetic order in this system unless there is a percolation connection between the sites on one of the four pairs of sublattices. For uncorrelated dilution this occurs at the same p_c as that of the nearest-neighbor percolation problem on a single isolated sublattice or on the entire lattice. For our problems the sublattices and the lattice itself have the same structure and coordination number, but this does not have to be true in general. For correlated dilution we conjecture that the critical threshold at p_c may bifurcate into critical thresholds $p_c^{(1)}, p_c^{(2)}, \ldots$, where $p_c^{(n)}$ is the threshold concentration above which percolation occurs on n sublattices. This separation of the thresholds leads to the possibility of order at an overall concentration below the usual percolation threshold on one or more of the four sublattices. An overall concentration above the usual threshold would be needed for all sublattices to order. If random exchange effects do not intervene, there would be order on, say, two sublattices, while the other sublattices remained disordered.

We consider the nature of the ground state when the sublattices are unequally populated. One may visualize the phase of the wave functions as being chosen as follows in the case when the correlation lengths ξ_i within the ith sublattice are all very different, say, $\xi_1 \gg \xi_4 \gg \xi_3 \gg \xi_2$. Consider a region of size ξ_1 and fix arbitrarily the phase on the cluster in sublattice 1 which spans the region. Now consider each connected cluster within any sublattice in order of decreasing size and determine the phase of its wave function. Essentially this means we consider first clusters on sublattice 1, then those on sublattice 4, and so forth, in view of the relative sizes of the ξ's. At each stage, the phase of a cluster will be determined by the exchange field due to the larger clusters within which it is embedded. Thus the correlation length ξ_i may be interpreted as the length scale over which the phase ϕ_i in the ith sublattice is constant. Thus, apart from an overall phase change ($\phi_i \to -\phi_i$ for all i), we have the following scenario. Over the shortest correlation length, ξ_2, the ground state is fixed. In regions of size ξ_3 the ground state will fluctuate between just two possibilities according to the sign of ϕ_2, which varies over the shorter length scale ξ_2. Likewise over regions of size ξ_4 (ξ_1) there will be 4 (8) ground states.

This scenario is illustrated in Fig. 4 for the case where ξ_1 and ξ_4 are larger than the size L of the sample shown, so that the phases of sublattices 1 and 4 have been fixed by considering the energetics on a length scale large com-

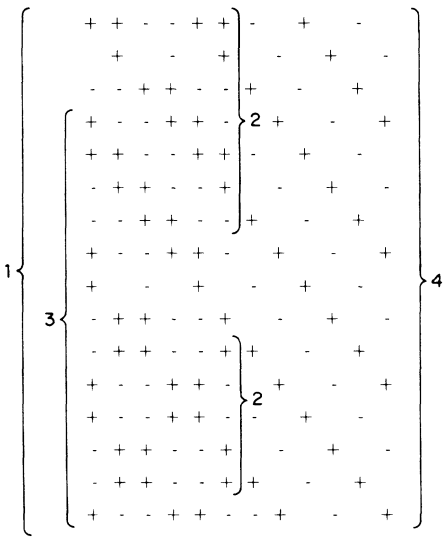

FIG. 4. Example of a ground-state configuration in the presence of correlated dilution. In the upper portion a staircase configuration is seen and in the lower a checkerboard state is selected. The sublattices are numbered as in Fig. 2. The correlation lengths within each sublattice are indicated by the braces, and are discussed in the text.

pared to L. Here ξ_3 is about 11 lattice spacings and ξ_2 about 6 or less spacings. We observe the following: Throughout the sample the two sublattices 1 and 4 are connected. In the upper part of the sample there is a region of some six spacings where all sublattices are connected and for the choice of phases selected here a staircase ground state is obtained. In the middle the connection on the sublattice 2 with a correlation length of only six spacings is broken. In the lower part of the sample the spins on sublattice 2 choose to take the other antiferromagnetic phase and a checkboard ground state is observed. We note that over this 18-spacing sample the choice of ground state is constrained to be one of two possibilities in the region where sublattices 1, 3, and 4 are connected. In general, when there is unequal occupation over some correlation length (possibly infinite, this would depend on the details of the system) the choice of ground states will always be reduced to some subset of the total number of ground states.

Conjectured zero-temperature phase diagrams for the dilute BNNNI with both random ($K=0$) and correlated dilution are given in Fig. 5. For concentrations, x, of magnetic atoms that fall below the K-dependent threshold, p_c^{NN+3NN}, for connectivity via either nearest-neighbor (NN) or third-nearest-neighbor (3NN) bonds, no order of any kind can be seen. We have calculated that in the absence of correlations $p_c^{NN+3NN}=0.338 \pm 0.004$ for the square lattice. This result is based on a finite-size scaling extrapolation from samples of up to 200×200 sites with periodic boundary conditions.

If $x > p_c^{NN+3NN}$, one might expect that spin-glass order sets in immediately. However, this is not the case due to frustration effects,[14] and we call the concentration at which spin-glass (SG) order does begin p_c^{SG}. One can understand the role of frustration from the following example. Consider the 2 sublattice PNNNI model. Here the K-dependent threshold below which no order can be seen is greater than or equal to p_c^{NN+2NN}, the threshold for connectivity via either NN or second-nearest-neighbor bonds. For $x > p_c^{NN+2NN}$ there can be configurations where two lines of connected points on different sublattices cross. If this occurs in the absence of further local connections then the crossing 2×2 square is frustrated and order cannot be transmitted from one sublattice to the other. Two possible orderings on such a dilution geometry are illustrated in Fig. 6. If such connections are deleted from the diluted system the concentration of occupied sites changes slightly and therefore $p_c^{SG} > p_c^{NN+2NN}$. For $p_c^{NN+2NN} < p_c^{SG} < x < p_c^{(1)} (p_c^{(1)} = p_c^{(n)} = p_c$, in the absence of correlations), there will be spin-glass order[9] if random exchange effects do not intervene. Partial order could occur in the regime $p_c^{(1)} < x < p_c^{(n)}$ and long-range order is only possible above $p_c^{(n)}$. Similar arguments apply for the BNNNI model except that here the lower threshold will be p_c^{NN+3NN}. We note that the frustration arguments are not relevant to the onset of long-range order. Here the frustrated connections play the role of a random field and an Imry-Ma argument can be developed to show that they do not destroy long-range order.

The implications of the potential hierarchy of correlation lengths in the partially ordered phase will be outlined in the conclusion and explored in depth in a future paper. For the remainder of this paper we shall be concerned with answering the more fundamental question of whether there exists more than one percolation threshold for systems with several sublattices and correlated dilution. To study this question we consider a correlated percolation model with two sublattices in the x-y plane which is suitable for either the BNNNI model or for the simpler PNNNI model. For the BNNNI model we would have one concentration for two of the four pairs of sublattices and another for the other two pairs. For the PNNNI each pair would have a potentially different concentration. Although the results of a percolation analysis will not be reliable in two dimensions, they may have qualitative validity for $d > 2$. Since the antiferromagnetic interaction is the dominant one, we will assume that two second nearest-neighboring sites, if occupied, are connected. The occupation of nearest neighbors is governed by correlations similar to those in a lattice gas. In this purely percolative model we ignore the effects of dilution-induced random exchange coupling between sublattices. Such an effect would reduce the probability of percolation, but would not affect the main issue, i.e., whether or not percolation can take place separately on one sublattice before percolation on both sublattices occurs. Because competing interactions are confined to a plane, we will study this percolation process numerically in two dimensions. To obtain a mean-field solution we start by considering this model on a Cayley tree.

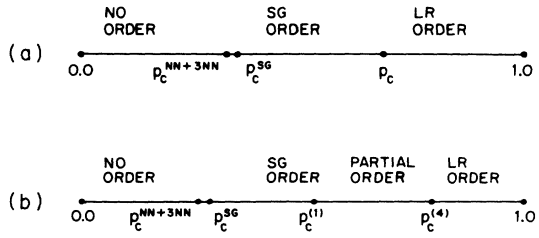

FIG. 5. Phase diagram for the BNNNI ($J^{\perp}\neq 0$) model with (a) random dilution, (b) correlated dilution, at zero temperature, as a function of concentration, p, for the case where there are different concentrations on each of the four pairs of sublattices. The thresholds, e.g., p_c^{NN+3NN} and p_c^{SG}, depend on the strength of the correlation K and are thus different in cases (a) and (b).

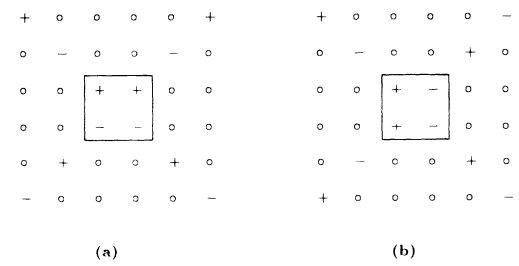

FIG. 6. A configuration in which order is not propagated through a frustrated square. When averaged over the two ground states (a) and (b); the phase of the top-left spins is uncorrelated with that of the bottom-left spins.

III. EXACT SOLUTION ON A CAYLEY TREE

We now consider the exact solution of the percolation model introduced in Sec. II on a two-sublattice Cayley tree. For that purpose we need to construct a generating or "partition" function from which we can determine whether or not percolation occurs on one or both sublattices. For the purposes of defining percolation we recall that we are interested in the propagation of long-range magnetic order in the PNNNI model. Therefore, we classify sites as being connected only with respect to second-neighbor linkages: i.e., two sites are in the same cluster if they are connected directly or indirectly via occupied sites with respect to second-neighbor linkages. Thus percolation depends only on the way sites in a given sublattice are occupied. Of course, the way such sites are occupied will depend on the compositional correlations introduced above. The nature of the compositional fluctuations in the presence of this repulsive interaction is formally identical to that of the antiferromagnetic lattice gas as studied on the Cayley tree by Murata.[10] Note that although Murata considered percolation in the presence of such lattice gas correlations, the percolation problem he considered is quite different from the one we are studying here. In particular, Murata considered the percolation via nearest neighbors in contrast to the percolation within sublattices, which to the best of our knowledge has not been previously considered. We will develop self-consistent equations for the percolation probability $P_\mu(p)$, on the μth sublattice.

The partition function Z we construct is a function of the chemical potential for occupation of an A site, μ_a, the chemical potential for occupation of a B site, μ_b, the percolation field, h, and the dimensionless repulsive energy, K, introduced above. The percolation field is used to identify A sites which are connected either directly or via intermediate A sites to the A site at the origin. We will treat the case where the origin is an A site and the Cayley tree is a two sublattice structure such that, except for boundary sites, each A site has $\sigma+1$ neighbors on B sites, and each B site has $\sigma+1$ neighbors on A sites. Thus

$$Z=\sum_C e^{-E(C)} , \tag{3a}$$

where the sum is over all configurations in which each site independently is occupied or not, and $E(C)$ is the "energy" associated with such a configuration, C. For $E(C)$ we write

$$E(C)=h\sum_j \nu(0,j)+K\sum_{\langle i,j\rangle}\epsilon_i\epsilon_j-\mu_a\sum_{i\in A}\epsilon_i-\mu_b\sum_{i\in B}\epsilon_i , \tag{3b}$$

where $\langle i,j\rangle$ indicates a sum over *pairs* of nearest-neighboring sites, ϵ_i is unity if site i is occupied and is zero otherwise, and $\nu(0,i)$ is unity if site i is connected by a path of occupied A sites to the A site at the origin and is zero, otherwise. The first term in Eq. (3b) may thus be written as hn_A, where n_A is the size of the cluster of A sites containing the origin. (If the origin is not occupied, $n_A=0$.)

To construct the partition function we start by writing the exact result for a tree having one generation, as shown in Fig. 7:

$$Z^{(1)}=e^{\mu_a-h}(e^{\mu_b-K}+1)^{\sigma+1}+(e^{\mu_b}+1)^{\sigma+1} , \tag{4}$$

which we write as

$$Z^{(1)}=e^{\mu_a-h}\Phi^{(1)}_{A+}(h)^{(\sigma+1)/\sigma}+\Phi^{(1)}_{A-}(0)^{(\sigma+1)/\sigma} , \tag{5}$$

where

$$\Phi^{(1)}_{A+}(h)=[e^{\mu_b-K}+1]^\sigma , \tag{6a}$$

$$\Phi^{(1)}_{A-}(h)=[e^{\mu_b}+1]^\sigma . \tag{6b}$$

Here $\Phi^{(k)}_{\mu\nu}(h)$ denotes the factor associated with a branch attached to a site with sublattice label μ (μ is either A or B) and occupation state ν, where ν is positive if the site is occupied and negative otherwise, and the superscript on Φ labels the generation. For the two generation tree shown in Fig. 7 we have

$$Z^{(2)}=e^{\mu_a-h}[e^{\mu_b-K}(e^{\mu_a-K-h}+1)^\sigma+(e^{\mu_a-h}+1)^\sigma]^{\sigma+1}+[e^{\mu_b}(e^{\mu_a-k}+1)^\sigma+(e^{\mu_a}+1)^\sigma]^{\sigma+1} , \tag{7}$$

which we may write as

$$Z^{(2)}=e^{\mu_a-h}\Phi^{(2)}_{A+}(h)^{(\sigma+1)/\sigma}+\Phi^{(2)}_{A-}(0)^{(\sigma+1)/\sigma} , \tag{8}$$

where

$$\Phi^{(2)}_{A+}(h)=[e^{\mu_b-K}\Phi^{(1)}_{B+}(h)+\Phi^{(1)}_{B-}(h)]^\sigma , \tag{9a}$$

$$\Phi^{(2)}_{A-}(0)=[e^{\mu_b}\Phi^{(1)}_{B+}(0)+\Phi^{(1)}_{B-}(0)]^\sigma , \tag{9b}$$

with

$$\Phi^{(1)}_{B+}(h)=[e^{\mu_a-K-h}+1]^\sigma , \tag{10a}$$

$$\Phi^{(1)}_{B-}(h)=[e^{\mu_a-h}+1]^\sigma . \tag{10b}$$

We generalize these results to a k-generation tree:

$$Z^{(k)}=e^{\mu_a-h}\Phi^{(k)}_{A+}(h)^{(\sigma+1)/\sigma}+\Phi^{(k)}_{A-}(0)^{(\sigma+1)/\sigma} , \tag{11}$$

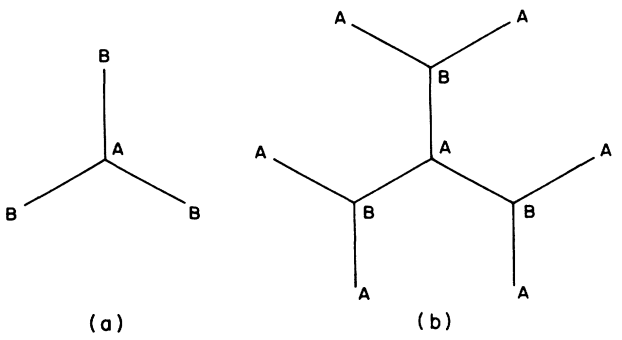

FIG. 7. Two-sublattice Cayley tree for $\sigma=2$ and with the origin on an A site, consisting of (a) one generation, (b) two generations.

with the Φ's determined by the recursion relations,

$$\Phi_{A+}^{(k)}(h)=[e^{\mu_b-K}\Phi_{B+}^{(k-1)}(h)+\Phi_{B-}^{(k-1)}(h)]^{\sigma}\ , \tag{12a}$$

$$\Phi_{A-}^{(k)}(0)=[e^{\mu_b}\Phi_{B+}^{(k-1)}(0)+\Phi_{B-}^{(k-1)}(0)]^{\sigma}\ , \tag{12b}$$

$$\Phi_{B+}^{(k)}(h)=[e^{\mu_a-K-h}\Phi_{A+}^{(k-1)}(h)+\Phi_{A-}^{(k-1)}(0)]^{\sigma}\ , \tag{12c}$$

$$\Phi_{B-}^{(k)}(h)=[e^{\mu_a-h}\Phi_{A+}^{(k-1)}(h)+\Phi_{A-}^{(k-1)}(0)]^{\sigma}\ , \tag{12d}$$

together with the boundary conditions,

$$\Phi_{A+}^{(1)}(h)=[e^{\mu_b-K}+1]^{\sigma}\ , \tag{13a}$$

$$\Phi_{A-}^{(1)}(0)=[e^{\mu_b}+1]^{\sigma}\ , \tag{13b}$$

$$\Phi_{B+}^{(1)}(h)=[e^{\mu_a-K-h}+1]^{\sigma}\ , \tag{13c}$$

$$\Phi_{B-}^{(1)}(h)=[e^{\mu_a-h}+1]^{\sigma}\ . \tag{13d}$$

We will study the recursion relations of Eq. (12) for an infinite-generation tree. For that purpose we set

$$\Phi_{B+}^{(k)}(h)/\Phi_{B-}^{(k)}(h)=\xi_B^{(k)}(h)\rightarrow\xi_B(h)\ , \tag{14a}$$

$$\Phi_{A+}^{(k)}(h)/\Phi_{A-}^{(k)}(0)=\xi_A^{(k)}(h)\rightarrow\xi_A(h)\ , \tag{14b}$$

$$\Phi_{B-}^{(k)}(h)/\phi_{A-}^{(k)}(0)=\eta^{(k)}(h)\rightarrow\eta(h)\ , \tag{14c}$$

where the limiting forms for $k\rightarrow\infty$ are indicated.

In terms of the limiting functions ξ and η the recursion relations are

$$\xi_A(h)=\left[\frac{\eta(h)[\xi_B(h)e^{\mu_b-K}+1]}{\eta(0)[\xi_B(0)e^{\mu_b}+1]}\right]^{\sigma}\ , \tag{15a}$$

$$\xi_B(h)=\left[\frac{\xi_A(h)e^{\mu_a-K-h}+1}{\xi_A(h)e^{\mu_a-h}+1}\right]^{\sigma} \tag{15b}$$

$$\eta(h)=\left[\frac{\xi_A(h)e^{\mu_a-h}+1}{\eta(0)[\xi_B(0)e^{\mu_b}+1]}\right]^{\sigma}\ . \tag{15c}$$

Solving Eq. (15c) we have

$$\frac{\eta(h)}{\eta(0)}=\left[\frac{\xi_A(h)e^{\mu_a-h}+1}{\xi_A(0)e^{\mu_a}+1}\right]^{\sigma}\ . \tag{16}$$

Using the solution and Eq. (15b), Eq. (15a) reduces to

$$\xi_A(h)-\left[\frac{e^{\mu_b-K}[\xi_A(h)e^{\mu_a-K-h}+1]^{\sigma}+[\xi_A(h)e^{\mu_a-h}+1]^{\sigma}}{e^{\mu_b}[\xi_A(0)e^{\mu_a-K}+1]^{\sigma}+[\xi_A(0)e^{\mu_a}+1]^{\sigma}}\right]^{\sigma}\equiv F(\xi_A(h),\xi_A(0),h)=0\ . \tag{17}$$

We will restrict ourselves to the case $\mu_a=\mu_b=\mu$. Then these equations should be solved in the following way. First, for $h=0$ one can solve Eqs. (17) to obtain $\xi_A(0)$ and, using Eq. (15b), $\xi_B(0)$. These solutions at zero field, h will reproduce the lattice-gas problem which results when no cluster information is retained (i.e., $h=0$). Then, having the solutions for $h=0$, one can proceed to solve Eq. (17) to get all the variables at nonzero field.

Before discussing the nature of the solutions, let us see what information they contain. Let us consider how one should determine the probability that an A site is occupied. For the Cayley tree to properly mimic a finite dimensional lattice, we should associate the probability that an A site is occupied, p_A, with the probability that the origin is occupied by an A site. In that way, we ensure that boundary effects (which are severe on the Cayley tree) vanish in the limit of infinite number of generations. Typically, the probability that a given site i is occupied is given by $\partial \ln Z/\partial\mu_i$, where μ_i is the chemical potential (in units of kT) for occupying site i. Here, although we have not introduced the necessary site-dependent chemical potentials, one can see that the explicit μ_a appearing in Eq. (11) is the chemical potential we should associate with the origin. This formulation should be used at $h=0$, since the purpose of the field is only to label clusters and not to modify the statistical weight. Thus we have

$$p_A^{(k)}=\frac{e^{\mu_a}\Phi_{A+}^{(k)}(0)^{(\sigma+1)/\sigma}}{e^{\mu_a}\Phi_{A+}^{(k)}(0)^{(\sigma+1)/\sigma}+\Phi_{A-}^{(k)}(0)^{(\sigma+1)/\sigma}}\rightarrow p_A$$
$$=\frac{\xi_A(0)^{(\sigma+1)/\sigma}e^{\mu_a}}{\xi_A(0)^{(\sigma+1)/\sigma}e^{\mu_a}+1}\ . \tag{18a}$$

Similar reasoning can be applied to the B sites, since for $h=0$ there is no distinction between sublattices:

$$p_B=\frac{\xi_B(0)^{(\sigma+1)/\sigma}e^{\mu_b}}{\xi_B(0)^{(\sigma+1)/\sigma}e^{\mu_b}+1}\ . \tag{18b}$$

From these equations one can eliminate μ_a and μ_b in favor of p_A and p_B (unless a first-order transition causes a region in p_A-p_B space to not correspond to a single-phase region.) In our treatment, where we set $\mu_A=\mu_B=\mu$, we can use Eq. (18) to express μ in terms of the average concentration $p=(p_A+p_B)/2$.

We can also determine the probability, P_{Af}, that the A site at the origin is occupied and is in a finite cluster of A sites. The quantity $1-P_{Af}$ is the order parameter in the ordinary (uncorrelated) percolation problem. To get P_{Af} note that for nonzero h a configuration in which the A site at the origin belongs to a cluster of n_A A sites, carries a relative weight $e^{-n_A h}$. Now we regard P_{Af} as be-

ing a fraction in which the denominator is a sum over the statistical weight of all configurations and the numerator as a sum over the statistical weight of only those configurations in which the origin is both occupied and in a *finite* cluster of A sites. The denominator is clearly $Z(0)$, since the normalization is determined by all configurations. In contrast, the numerator is the same as for p_A, except that here the limit $h \to 0^+$ should be taken to eliminate the infinite cluster. Thus we write

$$P_{Af}^{(k)} = \frac{e^{\mu_a}\Phi_{A+}^{(k)}(0^+)^{(\sigma+1)/\sigma}}{e^{\mu_a}\Phi_{A+}^{(k)}(0)^{(\sigma+1)/\sigma} + \Phi_{A-}^{(k)}(0)^{(\sigma+1)/\sigma}}$$

$$\to P_{Af} = p_A[\xi_A(0^+)/\xi_A(0)]^{(\sigma+1)/\sigma} . \tag{18c}$$

Consider first the properties of the $h=0$ solutions. Increasing the common chemical potential corresponds to increasing the concentration of the lattice gas with repulsive nearest-neighbor interactions. As is well known, there will be a range of K and μ over which this model exhibits phase separation. In this regime one finds solutions for which $\xi_A(0) \neq \xi_B(0)$. In this case we will choose the solution for which $\xi_A(0) > \xi_B(0)$, so that the A sublattice always has at least as high a density of occupation as the B sublattice. To study the percolative transition, one analyzes the solutions of Eq. (17) for nonzero h. Thereby one can obtain the quantity P_{Af} via Eq. (18c). From this one can determine the probability that an A site belong to an infinite cluster. It is apparent that percolation on the A sublattice occurs if and only if $\xi_A(0^+) \neq \xi_A(0)$, i.e., if and only if $\xi_A(h)$ depends discontinuously on h for $h \to 0$. One can also simultaneously obtain P_{Bf}, the probability that a finite cluster of B sites be formed. To obtain this quantity we must proceed indirectly, since we have not introduced a field to indicate to what cluster a B site belongs. For this purpose we now interchange A and B labels. Or equivalently, we consider the solution for which $\xi_A(0) < \xi_B(0)$. With this choice, $1 - P_{Af}$ will represent the probability that percolation occurs on the minority sublattice, originally labeled B.

Finally, we discuss the results of our calculations for the Cayley tree. First of all, when $K=0$ we should find the usual results for percolation on the A and B sublattices independently, with $p_A = p_B$. Since the branching ratio for a long path on a single sublattice is σ^2, we expect a percolative transition to occur when p_A (or p_B) equals σ^{-2}. For $K \neq 0$ we can find the limit of stability for a *continuous* percolation transition. (In principle, this transition can be preempted by a first-order transition if a lattice-gas ordering takes place before the continuous transition would occur.) We locate this instability by the condition that $\partial \xi_A(h)/\partial h = \infty$. In the notation of Eq. (17) this condition is

$$\left[-\frac{\partial F}{\partial h}\right]_{\xi_A(h),\xi_A(0)} \Big/ \left[\frac{\partial F}{\partial \xi_A(h)}\right]_{\xi_A(0),h} = \infty . \tag{19}$$

Since we are assuming no lattice-gas ordering, we now set $\xi_A(h) = \xi_B(h) \equiv \xi(h)$ and $h=0$. Then Eq. (19) can be written in terms of the variable $y = \xi(0)\exp(\mu)$ as

$$y = \frac{1}{\sigma^2 - 1} + \frac{\sigma^2}{\sigma^2 - 1}\frac{y^2 e^{-K}(1-e^{-K})}{(ye^{-K}+1)^2} . \tag{20}$$

For an arbitrary value of K this equation determines the value of y where the percolation susceptibility diverges (assuming no lattice-gas ordering). From this value of y we can obtain ξ using Eq. (15b), and thereby the value of μ, by $e^{\mu} = y/\xi$. Finally, using Eq. (18), we obtain the critical value of p as a function of K as $p_c(K) = y\xi^{1/\sigma}/(y\xi^{1/\sigma}+1)$. For instance, we consider the limiting cases, $K=0$ and $K=\infty$. In both cases, Eq. (20) gives $y = 1/(\sigma^2 - 1)$. Substituting $y = \xi\exp(\mu)$ into Eq. (15b) gives (for $\xi_A = \xi_B \equiv \xi$) $\xi = [\exp(-K) + \sigma^2 - 1]/\sigma^2$. Combining these results with Eq. (18a) we see that the threshold concentration for equal percolation on both sublattices is $p = \sigma^{-2}$ for $K=0$ and $p = (\sigma^2+1)^{-1}$ for $K=\infty$. The fact that these two thresholds are nearly equal explains why the instability line obtained from Eq. (20) and shown in Fig. 8 is almost independent of K.

Next we consider the phase boundary for lattice-gas ordering. Here we use the result of Murata:[10]

$$p_c = \tfrac{1}{2} \pm \tfrac{1}{2}\left[\left[\frac{(\sigma-1)^2}{(\sigma+1)^2} - e^{-K}\right] \Big/ (1-e^{-K})\right]^{1/2} . \tag{21}$$

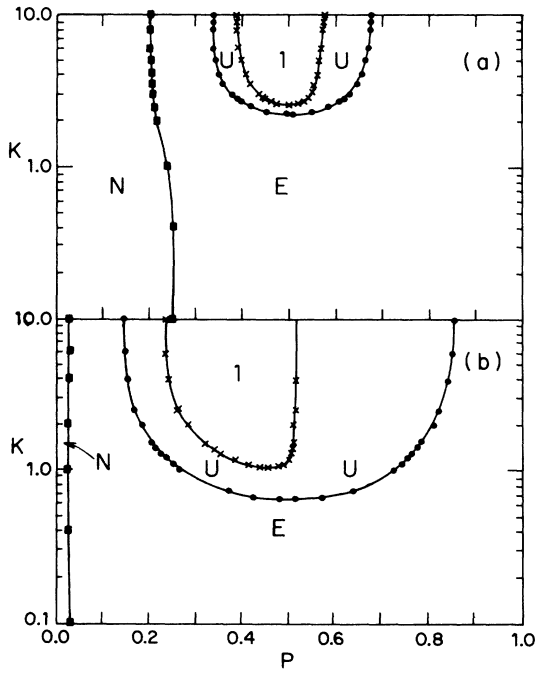

FIG. 8. Phase diagram for correlated percolation on a Cayley tree with two sublattices as a function of p and K. In regions N and E occupation is equal on both sublattices. In region N *neither* sublattice percolates, while in region E both sublattices percolate *equally*. In regions U and 1 there is unequal occupation on the two sublattices. In region U both sublattices percolate, but *unequally*, whereas in region 1 only *one* does. The points indicate the boundaries between the regions obtained from the solution of the self-consistent equations in sweeps across the phase diagram at constant K and varying chemical potential. The case of $\sigma=2$ is illustrated in (a) and that of $\sigma=6$ in (b).

This equation gives the boundary between the regions E and U in Fig. 8. Note that for $\sigma \geq 2$ the threshold of Eq. (20) for equal percolation and the lattice-gas ordering phase boundary of Eq. (21) do not intersect one another. For this case, no matter what the value of K, increasing the concentration, i.e., increasing the chemical potential, leads first to percolation equally on both sublattices and then, when K becomes large enough, to lattice-gas ordering. For $\sigma=1$ we have the case of one dimension, so that in this limit the size of the symmetric region around $p=\frac{1}{2}$ of lattice-gas ordering shrinks to zero. We have checked that even for σ infinitesimally greater than unity, the solution from Eq. (20) does not intersect the lattice-gas phase boundary. As we shall see, these two phase boundaries do meet in lower dimension. One can also determine exactly the concentration, P_{1-U}, of the higher concentration $1-U$ phase boundary at $K=\infty$. In this case when $p=\frac{1}{2}$ one sublattice will be completely filled, the other empty. Now percolation will take place on the minority sublattice when the concentration is raised above $\frac{1}{2}$ by an amount equal to the percolation threshold (at $p=p_c$) for random occupation on a single sublattice. (The occupation is random because there is no distinction in energy between sites on the minority sublattice.) This argument gives $p_{1-U}=(p_c+1)/2=(\sigma^2+1)/(2\sigma^2)$.

In Fig. 8 we show the four different regions in the phase diagram. There are the regions N and E where occupation is equal on both sublattices. In region N neither percolates whereas in region E they both do. In regions U and 1 the sublattices are unequally occupied (this is the two-phase region of the lattice gas). In region U both sublattices percolate, but unequally, whereas in region 1 percolation occurs only in one sublattice. To illustrate the behavior implied by this phase diagram, we show in Fig. 9 the variation of $P(p)$, the probability that a site is in an infinite cluster, for both sublattices versus p for $\sigma=2$ at fixed $K=3.5$.

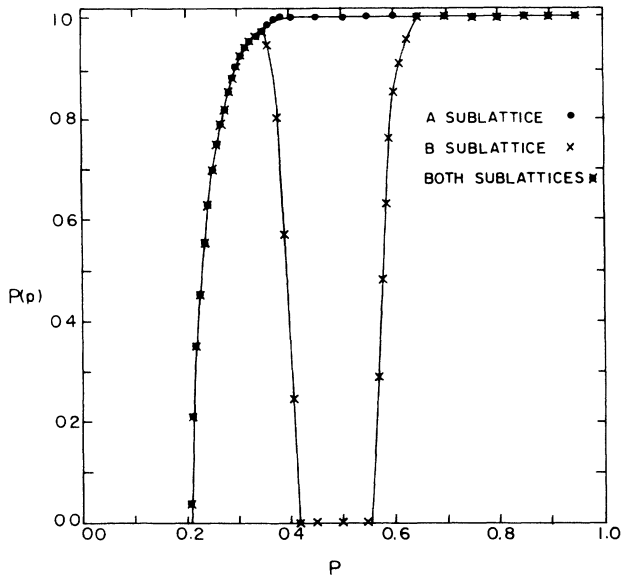

FIG. 9. Percolation probability $P(p)$ as a function of p on the two sublattices of a Cayley tree of $\sigma=2$ at $K=3.5$. The points indicate the values of $P(p)$ on each of the sublattices for a sweep of varying chemical potential.

IV. HAMILTONIAN FOR CORRELATED PERCOLATION

Here we give a Hamiltonian for correlated percolation, based on the ideas of Giri *et al.*[17] in their treatment of site percolation within a generalized Potts model. In principle we could modify the Potts lattice-gas Hamiltonian of Coniglio and Lubensky.[11] This would seem to require allowing some potentials to become infinite as done by Murata.[10] We avoid these complications. For this purpose we consider a two-colorable lattice, which for convenience we take to be a hypercubic lattice in d spatial dimensions with $d \geq 3$. We consider the case of a body-centered lattice in which the A sites are at positions $(l_1, l_2, \ldots, l_d)$, where l_k is an integer. The B sites form a similar simple hypercubic lattice with half-integral position components. Each lattice site has $2d$ nearest neighbors on its own sublattice at relative locations denoted $2\Delta_j$, for $j=1,2,\ldots,2d$. Each lattice site has 2^d neighbors on the other sublattice at relative locations $2\delta_j$, for $j=1,2,\ldots,2^{2d}$. (We include a factor of 2 in each of these definitions so that we can easily specify the midpoints of these relative neighbor vectors. Then following the idea of Giri *et al.*[17] we set

$$e^{-H}=\prod_{j\in A,B} e^{-H_j}, \tag{22}$$

where

$$e^{-H_j}=1-p+p\left[\prod_{\delta}(1+i\alpha\sigma_{j+\delta})\right]\left[\prod_{\Delta}\delta_{s_j,s_{j+\Delta}}\right], \tag{23}$$

where s_j is a q-state Potts variable which resides both on the midpoint of a bond joining two lattice sites in the *same* sublattice and on the sites themselves, and $\sigma_j=\pm 1$ is an Ising spin variable residing on the midpoint of a bond joining two lattice sites on *different* sublattices. Here p, the nominal concentration, plays a role analogous to the chemical potential and α plays a role comparable to the repulsive interaction K. For $\alpha=0$ one sees that this model is equivalent to two independent models for site percolation on the two sublattices. Thus the factor $1-p$ in Eq. (22) is associated with a vacant site and p with an occupied site. When a site is occupied the δ function in Eq. (23) forces the Potts variables at the site and on the bonds connected to the site to all be the same. Now consider the effect of the Ising spin variable when $\alpha\neq 0$. In taking the trace over the Ising variables the term $i\alpha\sigma_{j+\delta}$ can only contribute if it occurs twice, since $\mathrm{Tr}\sigma_{j+\delta}=0$. Thus for each pair of occupied nearest-neighboring sites on different sublattices the partition function includes a factor $(1-\alpha^2)\equiv e^{-K}$. As usual the limit when the number of Potts states goes to unity must be invoked to give the correct percolation weighting. In fact we might have married a q-state Potts model on the A sublattice with a q'-state Potts model on the B sublattice and considered the limit $q,q'\to 1$.

Now we must consider what kind of a field theory will result from this Hamiltonian. Recall that for site per-

colation, as Giri *et al.*[17] have shown, one obtains the usual Ψ^3 field theory:[18]

$$\mathcal{H}=\tfrac{1}{2}\sum_{\mu=1}^{q-1}\int d\mathbf{q}(r_0+q^2)\Psi_\mu(\mathbf{q})\Psi_\mu(-\mathbf{q}) + \tfrac{1}{6}u_3\sum_{\mu,\mu',\mu''}\int d\mathbf{q}_1\int d\mathbf{q}_2\lambda_{\mu,\mu',\mu''}\Psi_\mu(\mathbf{q}_1) \times\Psi_{\mu'}(\mathbf{q}_2)\Psi_{\mu''}(-\mathbf{q}_1-\mathbf{q}_2)\,, \tag{24}$$

where $\lambda_{\mu,\nu,\rho}$ is the characteristic form factor for cubic interactions in the Potts model. Here, since we have two sublattices, we will have, for $\alpha=0$, two independent such models involving Ψ and $\bar{\Psi}$. Now we discuss the effective Hamiltonian for small but nonzero α. Since for small α the lattice-gas ordering is far from criticality, we can imagine removing those degrees of freedom from the Hamiltonian representing the full correlated percolation model. Then we will be left with two Potts models modified by the small coupling terms introduced by having nonzero α. This coupling introduced by the Ising variable cannot involve contractions of the type $\sum_\mu\Psi_\mu\bar{\Psi}_\mu$, since, as we have noted, the number of states for the two sublattices can be different, although tending to unity. Thus the lowest-order interaction the correlation can introduce is of the form $\sum_{\mu,\nu}\Psi_\mu^2\bar{\Psi}_\nu^2$. Of course, the interaction can renormalize coefficients like r_0 and u_3, but such changes do not affect the universality class. The conclusion, since fourth-order potentials are irrelevant near $d=6$ dimensions, is that repulsion is irrelevant (at least when it is infinitesimal). Thus for small α (i.e., small K), we expect the same exponents for the percolation transition as in the absence of correlation. This conclusion agrees with that of Coniglio and Lubensky[11] for a related model. Interest therefore centers on the nature of the phase diagram near the lattice-gas transition line. As we shall see, there are various possible scenarios depending on dimension and possibly the coordination number and/or topology of the lattice.

V. RESULTS OF SIMULATIONS STUDIES FOR $d=2$

For the square lattice the simplest case is one where there are two equivalent interpenetrating sublattices. These are each made up of sites that are second neighbors of each other in the original lattice. We wish to compare the percolation behavior of the entire system with that of the two sublattices. If we introduce a nearest-neighbor repulsion this problem is equivalent to an antiferromagnetic Ising lattice gas as studied by Binder and Landau.[8] The temperature of their model corresponds to the annealing temperature in our case.

We have been able to extend one exact result from the Cayley tree to two dimensions. Here we can also claim that for the infinitely repulsive limit both sublattices will percolate above $p_{1-U}=(p_c+1)/2$. We have studied the square lattice by simulation of samples of L^2 sites with $L=10$, 20, 40, or 80. Initially, we considered different concentrations of occupied sites by randomly occupying sites with probability p and then allowing the system to equilibrate at some strength of correlation K by a Metropolis heat-bath relaxation with a repulsive lattice-gas interaction. We carried out this simulation at constant concentration (magnetization) by attempting movement of an occupied site from one sublattice to the other at each step. This is the so-called Kawasaki dynamics. In order to check that we had indeed achieved equilibrium we compared these results with relaxation at the same temperature but starting from a more ordered configuration. This "ordered" configuration was either ($p\le p_c$) random occupation on only one of the two sublattices but with probability $2p$, or ($p\ge p_c$) complete occupation on one sublattice and occupation with probability $2(p-0.5)$ on the other sublattice. For $L=10$ we found that equilibrium occurred at $K=1.0$ after $100L^2$ steps but for $L=40$ we found something like $500L^2$ steps were needed. We have considered different initial concentrations of $0\le p\le 1.0$ with emphasis on a medium correlation strength of $T=1.0$. For each concentration we considered at least 20 different lattices with each set of initial conditions, and sampled the data after each $100L^2$ attempted movements once equilibration was achieved.

A complete phase diagram for the $L=20$ system is given in Fig. 10. The solid line indicates the boundary of the sublattice ordered region of the lattice gas, as quoted from Binder and Landau.[19] This boundary is based on an extrapolation from samples of up to 80^2, with a different dynamics to ours. The dotted lines on the graph join points (indicated by open symbols) where 50% of the $L=20$ lattices or sublattices percolated. The diamonds indicate the points dividing the region N where no percolation occurs from a region of higher concentration where in 50% of the samples both sublattices are no

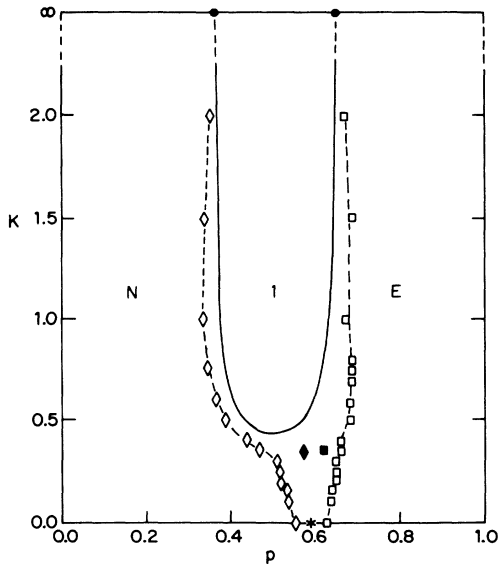

FIG. 10. Phase diagram for the correlated percolation model on a square lattice with two sublattices as a function of K and p. The regions are labeled as in Fig. 8. As explained in the text, the open symbols represent data from L^2 systems with $L=20$, whereas the solid symbols represent extrapolation to $L=\infty$ as illustrated in Fig. 11. The solid line is the lattice-gas phase boundary of Binder and Landau (Ref. 19).

longer disconnected. The squares indicate the points separating a region where, in 50% of the samples, both sublattices fail to be connected from region E where, in 50% at least of the samples, both sublattices are connected. For the $L=20$ samples we appear to have percolation on one sublattice only throughout the sublattice ordered regime. In the region between the lines, and well below the sublattice ordered region, there is a little of each kind of behavior and no indications that 50% or more of the lattices have any consistent result. Closer to the sublattice ordered region we have more than 50% of the samples with one sublattice only percolating and sublattice order. Thus there is an apparent outwards movement of the sublattice ordered region in all directions for the $L=20$ samples with Kawasaki dynamics relative to the results of Ref. 19.

In addition to the full phase diagram at $L=20$ we have considered larger samples for a selected value of K. The solid points on the graph indicate extrapolations from the larger samples using finite-size scaling, and are of course far more accurate than the $L=20$ results. The asterisk indicates the asymptotic critical threshold at $K=0$. Some details of the extrapolation are given in Fig. 11. Plots of two finite-size extrapolations for our system are given. The basis for these extrapolations is the finite-size scaling approach.[20] For the usual second-order percolation transition, we know that the width, $W(L)$, of the probability that a lattice of size L percolates at a concentration p, scales as $L^{-1/\nu}$, where ν is the correlation length critical exponent. $W(L)$ is measured by $p^L_{80}-p^L_{20}$ and a similar scaling is exhibited by $p^L_{50}-p_c$, where p^L_x is the concentration at which $x\%$ of samples of size L are connected in all directions. We plot p^L_{50} as a function of

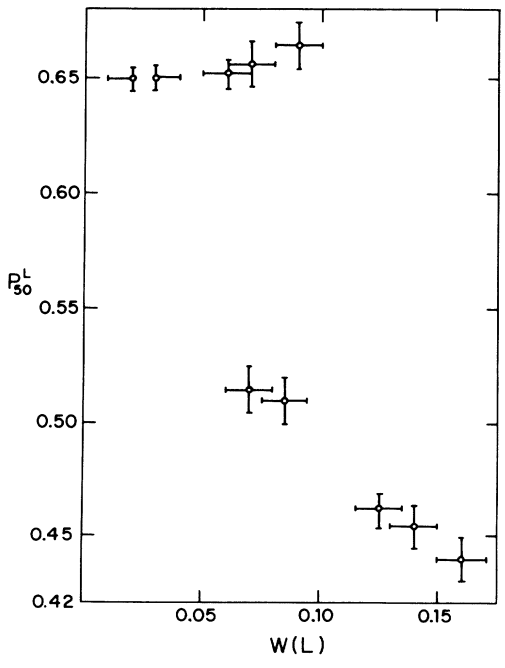

FIG. 11. Graph of p^L_{50} as a function of $W(L)$ for the two phase boundaries of Fig. 10 for L choices (right to left) of 10, 20, 30, 60, and 80.

$W(L)$ for $80\geq L\geq 10$ to determine p_c by extrapolation to $W(L)=0$ at $L=\infty$. The points on the graph are for L choices of 10, 20, 30, 60, and 80; the upper curve is for the square points that indicate the boundary of the E region, and the lower curve for the diamond points that indicate the boundary of the N region. We chose to make the detailed extrapolation at $K=0.35$ as it was here that there was a large difference between the end of the region in which neither sublattice percolated, and the beginning of the region in which they both do. We may observe from Fig. 11 that this gap is substantially decreased from a concentration difference in the p^{10}_{50}'s of about 0.22 to one of 0.14 in the p^{80}_{50}'s. Linear extrapolation to $L=\infty$ reduces it still further to about 0.04. We cannot claim that within our error bars (which are based on statistical errors) it is zero, although an extrapolation of the $L=10$, 20, and 30 data would have given this. We may have underestimated the systematic error in the dynamics for the larger samples, and discuss the detailed behavior of the largest samples to elaborate on this. At $K=0.35$ for $L=80$ as a function of increasing average concentration, we move from region N to a region where one sublattice percolates in more than 50% of the samples, just as for the smaller samples, and region 1 of the Cayley tree. However, at still higher concentration, both sublattices percolate although there is no overall percolation (i.e., with respect to nearest-neighbor connections.) From examinations of pictures of the samples we believe that this percolation of both sublattices without overall percolation may not be a region of the type U as seen on the Cayley tree but could be indicative of phase separation. This is plausible since in two dimensions the interface is not stable. We expect that if we could wait long enough we would find region-1 behavior. We are unable to prove this contention, but note that even if the region of both sublattices percolating without overall percolation is stable for infinite systems, it still differs from region U on the Cayley tree, since in region U there is overall percolation. The two possible scenarios are indicated in Fig. 12. In Fig. 12(a) we illustrate the situation where only regions N, 1, and E are present, and in Fig. 12(b) the case where there is a region with two sublattices percolating but no overall connection is present.

If our contention about the absence of region U is correct and we do interpret these results to imply that in this phase diagram region U has disappeared, then this is something of a surprise. We did not expect to see this region below p_c of the uncorrelated system, because if the lattices show different behavior then the occupation density of the less preferred one is below p_c, and we would not expect it to percolate if it is so highly dilute. However, we would expect to see it in general at the right of the two phase region. We suspect that the reason it may not occur here is that the bound $0.5+0.5p_c$ above which both sublattices must percolate is above the zero-temperature boundary of the two-phase region at $p=0.645$ (Ref. 19), and that it would be seen in a similar model on a lattice with $p_c\leq 0.5$. Consideration of such systems will be deferred to a later work.

We summarize the two-dimensional results as follows. The main result that we have successfully demonstrated

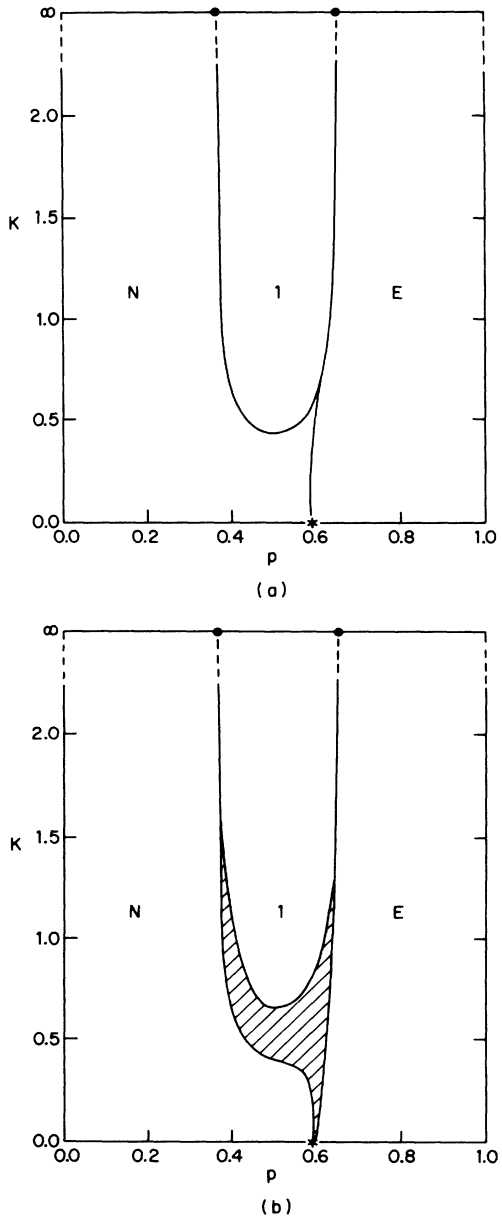

FIG. 12. Topology of the phase diagram for the scenarios. (a) Phase separation occurs, but there is no U region where both sublattices percolate, but unequally, and (b) such a region does occur in which both sublattices percolate unequally. The regions are labeled as in Fig. 8.

is the presence of a region where there is a percolation on only one of the two sublattices. This region occurs for concentrations below the threshold of the uncorrelated system, and is analogous to region 1 on the Cayley tree. Percolation in the entire system begins at a threshold that is higher than the uncorrelated one. In addition, we have suggested that the region U, if present, is of a different type to that seen on the Cayley tree.

VI. CONCLUSIONS

We argued in Sec. II that the critical threshold at p_c may bifurcate into multiple thresholds when correlations are introduced into the dilution of a BNNNI or PNNNI model. Thus correlated dilution can lead to novel phases with percolation on some but not all sublattices for Cayley trees, and for the square lattice in two dimensions. It would be reasonable to interpolate from this that such phases will occur for other (notably three) dimensions. We have, however, found certain differences between the two-dimensional and Cayley-tree phase diagrams, and further calculations will be required to determine the details of the correct phase diagram for other lattices and dimensions. In particular, it is not yet clear if there will be a phase of the type labeled U in Fig. 8 where both sublattices percolate, but do so unequally, for finite dimensional systems. We suspect that such a phase may be seen for those cases where $p_c \leq 0.5$. There is also the possibility that consideration of systems with more than two differentially occupied sublattices will lead to further topologies in the phase diagrams.

Let us now consider the implications of these different percolation phases for the correlated dilute BNNNI and PNNNI models, and the spin-glass systems that they model. We note that our models are intended to resemble the phase diagrams of real spin glasses as a function of the concentration of the nonmagnetic dilutant, to approximately the same degree as the two-dimensional Ising system resembles a three-dimensional single domain of Fe or the three-state Potts antiferromagnet on the triangular lattice[7] resembles the ortho-para hydrogen system.[8] In other words, we expect that the topology of the phase diagram should be the same but that critical exponents, locations of transitions, and relative areas of different phases could be very different.

For a range of dilutant concentrations, representation on this level has to date only been achieved from a microscopic model for the insulating glasses with models of the type of Ref. 13. These models are very similar to ours; the difference lying in the fact that our pure model has a multisublattice ordered state. Therefore, unlike a model that has a ferromagnetic ground state in the pure limit, where correlations in the dilution do not change the topology of the phase diagram, in our cases correlations in the dilution can open out the zero-temperature spin-glass–long-range order boundary at $x = p_c$ into a region of partial order $p_c^{(1)} x < p_c^{(n)}$. In this partially ordered region there would be a whole hierachy of correlation lengths on different sublattices. We think that this region corresponds to the region existing in some metallic glasses,[3] characterized by interactions between larger modulated regions and smaller ferromagnetic regions. Cable *et al.*[3] have suggested that "the interactions between these . . . regions are an essential element in understanding the complicated magnentic behavior of this (Cu-Mn) spin-glass system." We suggest that further exploration of our partially ordered region at finite temperatures will lead towards an understanding of the interactions between these regions since both are present in our model as a direct results of our microscopic interactions. We do not see how much simpler microscopic interactions could give both regions. We note that certain details of our model differ from those in Cu-Mn, in principle, since we have ferromagnetic nearest and antiferro-

magnetic further neighbor interactions, whereas Cu-Mn may have the opposite.[3] This simply means that we expect that our short-range order will be antiferromagnetic whereas in Cu-Mn it is ferromagnetic. The nature of the interplay between the short-range order and the long-ranged modulated order should be similar in both cases, and therefore study of our models could shed light on this interesting question.

The partially ordered phase bears some resemblance to the region of concentration immediately below that sufficient for long-range order in the three-state Potts antiferromagnet on the triangular lattice which has analogies with the ortho-para hydrogen system. In such a case the correlation length is locally different on different sublattices for reasons of geometry, and there is a higher degree of local order than in a usual spin-glass picture. There may or may not be a finite-temperature glass freezing transition in these systems. In all three cases the systems are not unlike the old superparamagnetic spin-glass models,[21] but these neglected the possibility of interactions between the different regions and in our models there is a natural source for such interactions through the microscopic connections. If any of these cases is considered to be somewhat like an interacting superparamagnetic cluster model, then it could be viewed[22] as a renormalized Edwards-Anderson model. For the metallic glasses we suggest that certain details that are lost in such a renormalization are important for the understanding of the mixed phase. However, this interpretation leads us to believe that our BNNNI and PNNNI models will give correct spin-glass properties for finite temperatures at the lower concentrations of magnetic species.

Consideration of the finite-temperature behavior will be made in a future paper, but we conjecture that the zero-temperature phase diagrams presented in Fig. 5 will also be correct for small finite temperatures for $d>2$. For $p_c^{\mathrm{NN+3NN}}<p_c^{\mathrm{SG}}<x<p_c^{(1)}$ the system will feel some stiffness and will be rather like the spin-glass phase of the model of Ref. 13. As long as there is no percolation on any of the sublattices, the modulated order will not persist over large distances. In the regime $p_c^{(1)}<x<p_c^{(n)}$ there will be short-ranged antiferromagnetic regions and longer-ranged modulated order, and for $x>p_c^{(n)}$ there will be long-range modulated order. We expect that thermal fluctuations may give rise to a reentrance of the spin-glass–long-range order boundary.

After completing these calculations we obtained a copy of a paper[23] that independently develops the Imry-Ma arguments of Sec. II.

ACKNOWLEDGMENTS

This work was supported in part by grants from the Israel Academy of Sciences and Humanities, and by the U.S.–Israel Binational Science Foundation. Also A.B.H. acknowledges partial support from the Materials Research Laboratory (MRL) program of the National Science Foundation under Grant No. DMR 85-19059. One of us, A.C.D.v.E, was supported by the Lady Davis Foundation. We thank R. G. Palmer for comments on a draft of this work, P. Monod for a talk that introduced one of us (J.A.) to the experimental works on this subject, and J. A. Mydosh for useful correspondence on the importance of positional correlations. The support and encouragement of A. Aharony, S. Fishman, and J. Avron during this calculation is much appreciated.

[1]K. Binder and A. P. Young, Rev. Mod. Phys. **58**, 801 (1986).
[2]A. F. J. Morgownik, G. J. Nieuwenhuys, J. A. Mydosh, and C. van Dijk, J. Phys. F. **17**, 199 (1987).
[3]J. W. Cable, S. A. Werner, G. P. Felcher, and N. Wakabayashi, Phys. Rev. Lett. **49**, 829 (1982); J. W. Cable, S. A. Werner, G. P. Felcher, and N. Wakabayashi, Phys. Rev. B **29**, 1268 (1984).
[4]A. F. J. Morgownik and J. A. Mydosh, Solid State Commun. **47**, 325 (1983).
[5]D. P. Landau and K. Binder, Phys. Rev. B **31**, 5946 (1985).
[6]J. Oitmaa and M. J. Velgakis, J. Phys. A **20**, 1495 (1987), and references therein.
[7]J. Adler, R. G. Palmer, and H. M. Meyer, Phys. Rev. Lett. **58**, 882 (1987).
[8]A. B. Harris and H. Meyer, Can. J. Phys. **63**, 3 (1985); **64**, 890 (1986).
[9]J. Adler, A. C. D. van Enter, and A. B. Harris, Bull. I.P.S. **33**, 113, (1987).
[10]K. K. Murata, J. Phys. A **12**, 81 (1979).
[11]A. Coniglio and T. C. Lubensky, J. Phys. A **13**, 1783, (1979).
[12]E. Rastelli, A. Tassi, and L. Reatto, Physica B **97**, 1 (1979).
[13]K. Binder, W. Kinzel, and D. Stauffer, Z. Phys. B **36**, 161 (1979).
[14]A. B. Harris, J. Phys. A **20**, L1011 (1987).
[15]P. Bak, S. Coppersmith, Y. Shapir, S. Fishman, and J. Yeomans, J. Phys. C **18**, 3911 (1983).
[16]Y. Imry and S.-K. Ma, Phys. Rev. Lett. **35**, 1399 (1975).
[17]M. R. Giri, M. J. Stephen, and G. S. Grest, Phys. Rev. B **16**, 4971 (1977).
[18]A. B. Harris, T. C. Lubensky, W. K. Holcomb, and C. Dasgupta, Phys. Rev. Lett. **35**, 327 (1975); **35**, 1397(E) (1975).
[19]K. Binder and D. P. Landau, Phys. Rev. B **21**, 1941 (1980).
[20]D. Stauffer, *Introduction to Percolation Theory* (Taylor and Francis, London, 1985).
[21]L. E. Wenger and J. A. Mydosh, Phys. Rev. B **29**, 4156 (1984).
[22]Reference 1, p. 861.
[23]J. F. Fernandez, Europhys. Lett. **5**, 129 (1988).